Pure Appl. Geophys. 168 (2011), 1951–1961

DOI 10.1007/s00024-011-0280-8

Pure and Applied Geophysics

Sedimentary Deposits from the 17 July 2006 Western Java Tsunami, Indonesia: Use of Grain Size Analyses to Assess Tsunami Flow Depth, Speed, and Traction Carpet Characteristics

Andrew Moore,[1] James Goff,[2] Brian G. McAdoo,[3] Hermann M. Fritz,[4] Aditya Gusman,[5] Nikos Kalligeris,[6] Kenia Kalsum,[5] Arif Susanto,[7] Debora Suteja,[5] and Costas E. Synolakis[8]

Abstract—The 2006 western Java tsunami deposited a discontinuous sheet of sand up to 20 cm thick, flooded coastal southern Java to a depth of at least 8 m and inundated up to 1 km inland. In most places the primarily heavy mineral sand sheet is normally graded, and in some it contains complex internal stratigraphy. Structures within the sand sheet probably record the passage of up to two individual waves, a point noted in eyewitness accounts. We studied the 2006 tsunami deposits in detail along a flow parallel transect about 750 m long, 15 km east of Cilacap. The tsunami deposit first becomes discernable from the underlying sediment 70 m from the shoreline. From 75 to 300 m inland the deposit has been laid down in rice paddies, and maintains a thickness of 10–20 cm. Landward of 300 m the deposit thins dramatically, reaching 1 mm by 450 m inland. From 450 m to the edge of deposition (around 700 m inland) the deposit remains <1 mm thick. Deposition generally attended inundation—along the transect, the tsunami deposited sand to within about 40 m of the inundation limit. The thicker part of the deposit contains primarily sand indistinguishable from that found on the beach 3 weeks after the event, but after about 450 m (and roughly coinciding with the decrease in thickness) the tsunami sediment shifts to become more like the underlying paddy soil than the beach sand. Grain sizes within the deposit tend to fine upward and landward, although overall upward fining takes place in two discrete pulses, with an initial section of inverse grading followed by a section of normal grading. The two inversely graded sections are also density graded, with denser grains at the base, and less dense grains at the top. The two normally graded sections show no trends in density. The inversely graded sections show high density sediment to the base and become less dense upward and represents traction carpet flows at the base of the tsunami. These are suggestive of high shear rates in the flow. Because of the grain sorting in the traction carpet, the landward-fining trends usually seen in tsunami deposits are masked, although lateral changes of mean sediment grain size along the transect do show overall landward fining, with more variation as the deposit tapers off. The deposit is also thicker in the more seaward portions than would be produced by tsunamis lacking traction carpets.

Key words: Tsunami deposit, Java, traction carpet.

1. Introduction

The 2006 western Java tsunami provides a rare opportunity to study the deposits of a moderate tsunami along a relatively low profile beach-ridge plain on which the intervening swales are occupied by rice paddies. These tsunami deposits provide important information regarding flow dynamics not available from other field evidence of the flow. This region is well suited for this study as tsunami deposits are easily distinguished from the soils on which they rest, and the low relief coastline of much of the Java coast allows the tsunamis to dissipate inland rather than rushing up steep hillsides.

Tsunami sedimentation has been studied for several smaller modern tsunamis, including 1992 Flores (Minoura *et al.,* 1997; Shi *et al.,* 1995), 1993 Okushiri (Nishimura and Miyaji, 1995; Sato *et al.,* 1995), 1994 Java (Dawson *et al.,* 1996), 1998 Papua New Guinea (Gelfenbaum and Jaffe, 2003), 2009 South Pacific (Dominey-Howes and Thaman, 2009), and also the

[1] Department of Geology, Earlham College, Richmond, IN 47374, USA. E-mail: moorean@earlham.edu
[2] Australian Tsunami Research Centre, School of Biological, Earth and Environmental Sciences, University of New South Wales, Sydney, NSW 2052, Australia. E-mail: j.goff@unsw.edu.au
[3] Department of Geology and Geography, Vassar College, Poughkeepsie, NY 12604, USA. E-mail: brmcadoo@vassar.edu
[4] School of Civil and Environmental Engineering, Georgia Institute of Technology, Savannah, GA 31407, USA. E-mail: fritz@gatech.edu
[5] Department of Oceanography, Institute of Technology Bandung, Bandung 40132, Indonesia.
[6] Department of Environmental Engineering, Technical Universtity of Crete, 73100 Chanea, Greece.
[7] Department of Geology, Institute of Technology Bandung, Bandung 40132, Indonesia.
[8] Tsunami Research Center, Viterbi School of Engineering, Los Angeles, CA 90089, USA. E-mail: costas@usc.edu

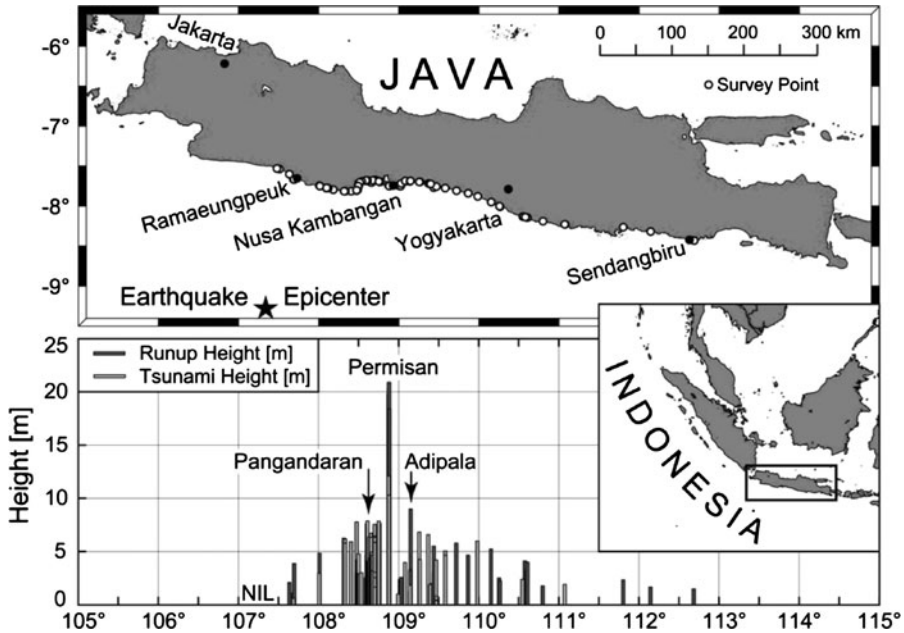

Figure 1
Measured tsunami runup and tsunami heights along Java's south coast (Fritz *et al*., 2007). Located epicenter for the 17 July 2006 earthquake relative to the study area at Adipala. Tsunami height is composed of terrain elevation and flow depth above ground

great 2004 Indian Ocean Tsunami (e.g., Paris *et al.,* 2009; Bahlburg and Weiss, 2007; Moore *et al.,* 2006). The 2006 Western Java tsunami provides a simple test case for testing ideas about the nature of tsunami sedimentation and how these deposits relate to flow dynamics.

In the modern environment, it is possible to relate the structures and properties of tsunami deposits with estimates of flow depth based on eyewitness accounts and post-tsunami surveys. These relationships, in turn, help determine the size of ancient tsunamis using the sedimentary record (Jaffe and Gelfenbaum, 2007; Moore *et al.,* 2007). Deposits from the 2006 Western Java tsunami may be used to test these ideas because their depositional patterns are minimally affected by local cross-shore or longshore topography, and because they include a wide range of grain sizes to record horizontal and vertical changes in the deposit.

2. *The 2006 Earthquake and Tsunami*

At 08:19 UTC on 17 July 2006, an earthquake estimated at Mw = 7.8 resulted from a ~200 km-long rupture of the fault boundary between the subducting Australian Plate and the overriding Eurasian Plate (Bilek and Engdahl, 2007; Fujii and Satake, 2006). Although few people felt this "slow" earthquake, with a low moment to energy ratio (Reymond, 2006; Newman, 1998), the resulting tsunami affected at least 200 km of coastline and ran up more than 20 m locally, killing more than 600 people (Fritz *et al*., 2007).

An International Tsunami Survey Team composed of tsunami researchers from Greece, Indonesia, New Zealand, Norway, and the United States visited the damaged area from August 3rd to 7th, 2006, in order to survey the damage caused by the tsunami (Fritz *et al*., 2007). The 17 members formed five teams specializing in runup (three teams), greenbelt effectiveness, and sedimentation. The sedimentology team wrote this paper.

The sedimentology team traveled primarily to coastal lowlands where the runup teams and satellite imagery suggested extensive sand deposition. Coastal plains extending inland for at least 1 km are common along ~30 km of coastline centered on Pangandaran (Fig. 1), and for 50 km east of Cilacap. Between the two cities and west of the Pangandaran plain the

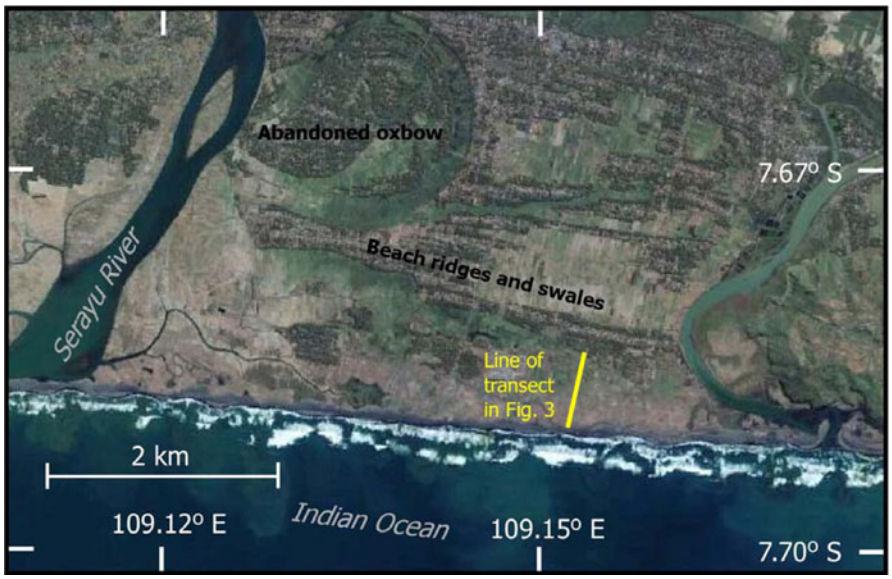

Figure 2
2003 GeoEye photo of the study area showing line of transect in Fig. 3 (Photo credit: Google Earth)

coastline becomes steep, limiting the possibility of sediment deposition.

3. Adipala Study Area

We selected the Adipala study area, east of Cilacap, because of its relatively uniform physiography with few buildings, ease of access and presence of abundant flow direction indicators in the form of low-lying dune grasses and rice plants. In this location we characterized the tsunami sedimentation by establishing a measured transect in the direction of flow, extending from the shoreline to the limit of inundation.

The 750 m transect is located between the Serayu and Bengawan rivers, about 15 km east of Cilacap (Fig. 2). It lies on an open coastal plain with Holocene beach and dune sands overlying Tertiary andesitic breccias (Asikin *et al.,* 1992). The first 80 m from the mean high tide (MHT) line is the modern beach ridge with an elevation of 1.2 m above MHT. With the exception of a narrow ridge and swale topography, the remainder of the transect passes through a generally broad, flat plain that has been terraced for rice farming, gaining ~20–50 cm of elevation between dikes that separate individual rice paddy fields which are practically flat, and vary in length between 15 and 60 m (along the transect) and are 15–20 m wide (Fig. 3).

Although few markers of flow depth were available along the transect, eyewitnesses to the disaster reported that the tsunami here reached flow depths of 5 m adjacent to the coast, and that large waves arrived twice, with the second wave being larger than the first. The eyewitness observations in Adipala fit well with the regional observations made by Fritz *et al.*, (2007), where the wave height averaged around 5 m for ~100 km east of Cilicap.

4. Methods

Our measured transect originates at the shoreline at 7°41′25.5″S, 109°8′51.6″E and extends ~755 m inland in the direction of flow, crossing the inland limit of tsunami-deposited sand around 720 m from shore and extending 40 m farther to the limit of inundation (Fig. 3). We surveyed topography with a hand level and tape measure. The horizontal distance between stations was kept to <5 m (to retain accuracy). We measured sediment thickness, described deposit stratigraphy, and collected sediment samples at 20–40 m intervals along this transect. Sampling

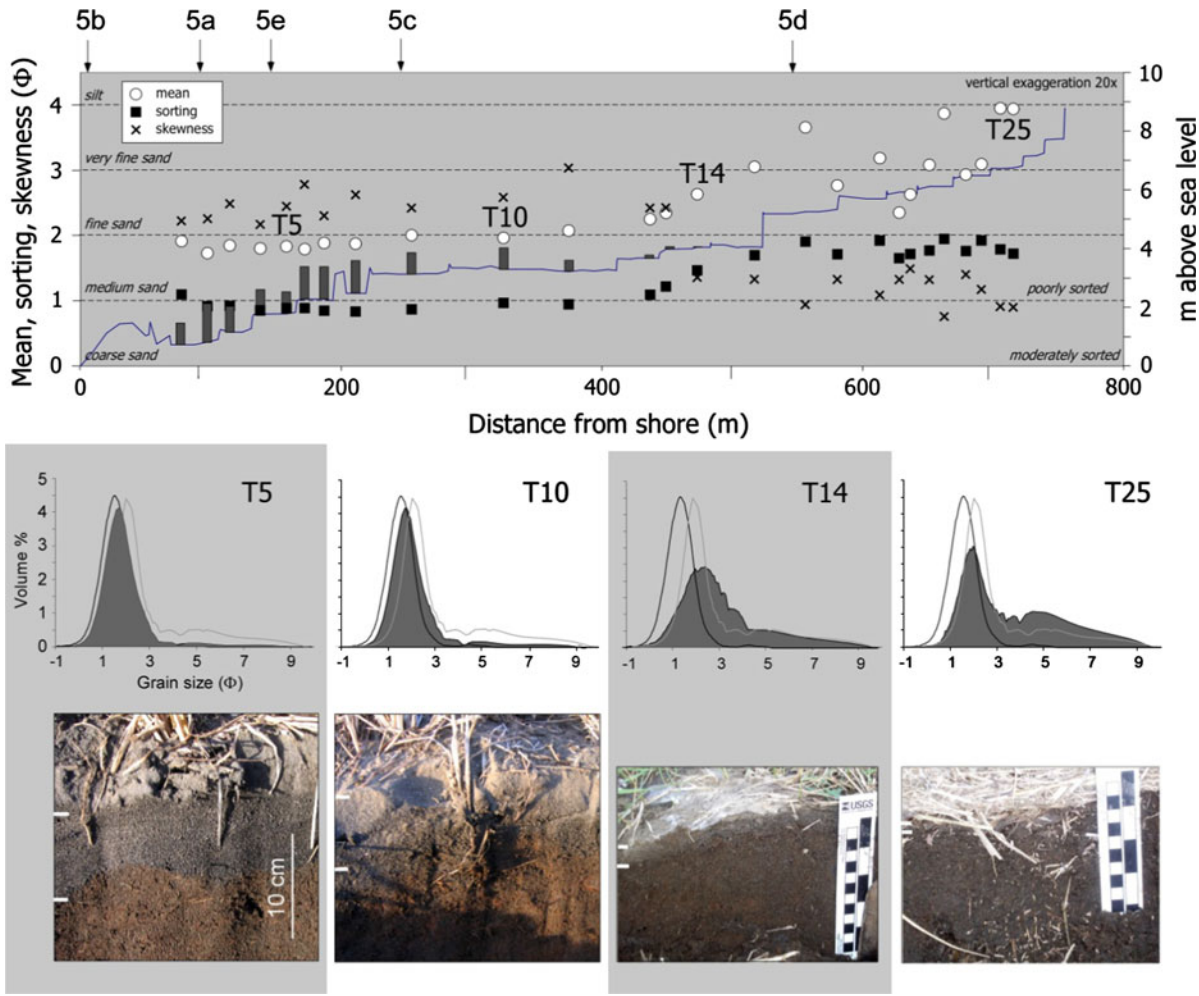

Figure 3

Sediment transect at Adipala, central Java. *Upper half* transect topography measured using a hand level and measuring tape, with the sediment grain size mean, standard deviation, and skewness overlain. Where more than one sample of the deposit was taken, the moment calculation is based on a weighted average of the samples. The deposit thickness is shown as a *vertical bar* on the topographic profile. *Lower half*. Grain size (in Φ) profiles for samples T5, T10, T14 and T25 are representative of the four zones of sediment deposition. The *gray shaded* region is the grain size profile for the sample, the black outline is the grain size profile of beach sand, and the gray outline is the grain size profile of soil underlying the tsunami deposit. Photographs of in situ deposits correspond to where samples T5, T10, T14 and T25 were taken

locations were determined so that at least one sample was collected from each diked field along the transect, and so that no sampling location was located close to a dike, where the localized increased turbulence might overwhelm the overall trends in sedimentology and stratigraphy that are representative of the larger-scale flow dynamics of the tsunami. Additionally, 100 m from the shore we pushed a 50 cm plastic core tube vertically through the deposit. The sediment was retained in the tube and subsequently opened in the laboratory. Grain size analyses of sub-samples taken at 0.5 cm intervals document the vertical grain size changes in the deposit.

Samples for grain size analysis were dry heated to 140°C for 48 h before analysis. Few organics were present in the sand samples (<1% by volume for most samples, ~10% by volume for the most landward samples); large organic debris (primarily rice stems) was removed with a forceps. Although seaward samples contained almost no silt or clay, landward samples often had abundant silt (up to 55% by volume).

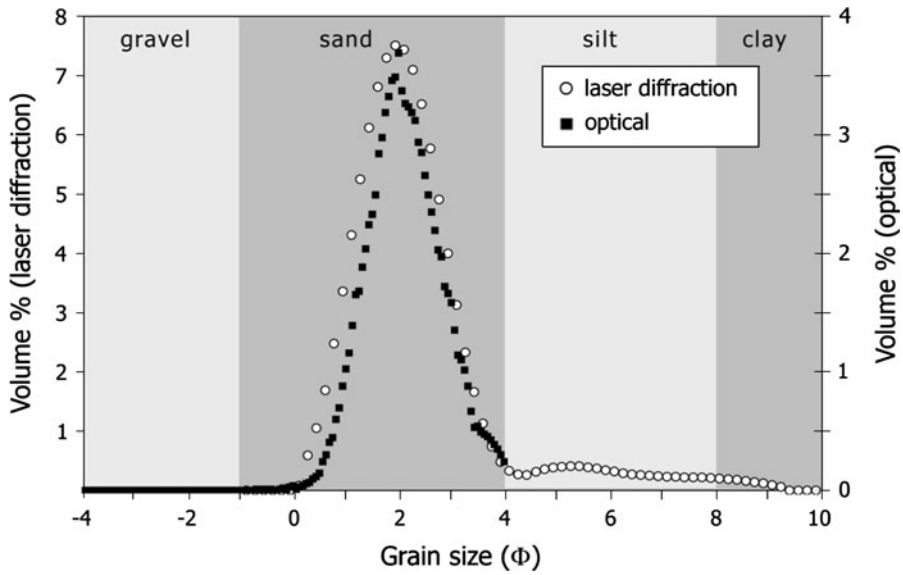

Figure 4
Comparison of grain size data of the same sample using both laser diffraction and optical methods. The mode is indistinguishable at the output resolution of each machine (1/6 Φ for laser diffraction, 1/16 Φ for optical). The change in vertical scale is caused by the differing resolutions of the two methods

We determined grain size within the deposit using a Retsch Camsizer, an optically based instrument capable of determining grain size to within ±1% over the range 30–30,000 μm (~5 to −5 Φ). The instrument images a falling curtain of sediment at 25 Hz, then determines the grain size of each particle in the image, in our case by determining the cross-sectional area of the particle and then reporting the diameter of a circle of equivalent area. The instrument made between 10 and 30 million individual measurements on our samples (depending on sample size) allowing resolution of 1/16–1/32 Φ. To resolve trends in material finer than 5 Φ, we also ran a split of the samples using laser diffraction (Malvern Mastersizer 2000) to measure grain size, resolving 1/6 Φ intervals from −1 to 15 Φ. Each dataset shows a main peak at ~1.5 Φ, with the Malvern and Camsizer peaks indistinguishable from each other at their respective resolutions (Fig. 4). Accordingly, we joined the two curves by normalizing to the main peak height, then using Camsizer data for material coarser than 4 Φ (taking advantage of the Camsizer's increased resolution in this range), and using Malvern data for material finer than 4 Φ (to take advantage of the Malvern's extended range). Sample mean and standard deviation were determined using the method of moments on data from the combined dataset, whereas median grain size was determined by linear interpolation.

5. Transect Description

The beach at Adipala is 30–40 m wide and has an overall slope of ~0.05. Breakers offshore generally spill, suggesting that the beach profile reflects dissipative, low to moderate energy conditions (Fig. 5a, b). These traits suggest that the profile is appropriate for the observed energy conditions—therefore either the tsunami did not significantly affect the beach morphology or the beach had re-equilibrated in the 3 weeks between the tsunami and our study.

The transect begins at the landward edge of the beach, which is marked by a 1 m-high coastal dune that grades into a ridge and swale topography (3 ridges, 2 swales) before being reformed into rice paddy fields 25 m past the base of the last ridge, 1 m above sea level. These terraced rice fields, separated by narrow earthen dikes, extend 700 m inland (9 m above sea level) to a plantation of palms and the start of a major, broad (~250 m), wooded ridge that extends the distance between the Serayu and Bengawan rivers.

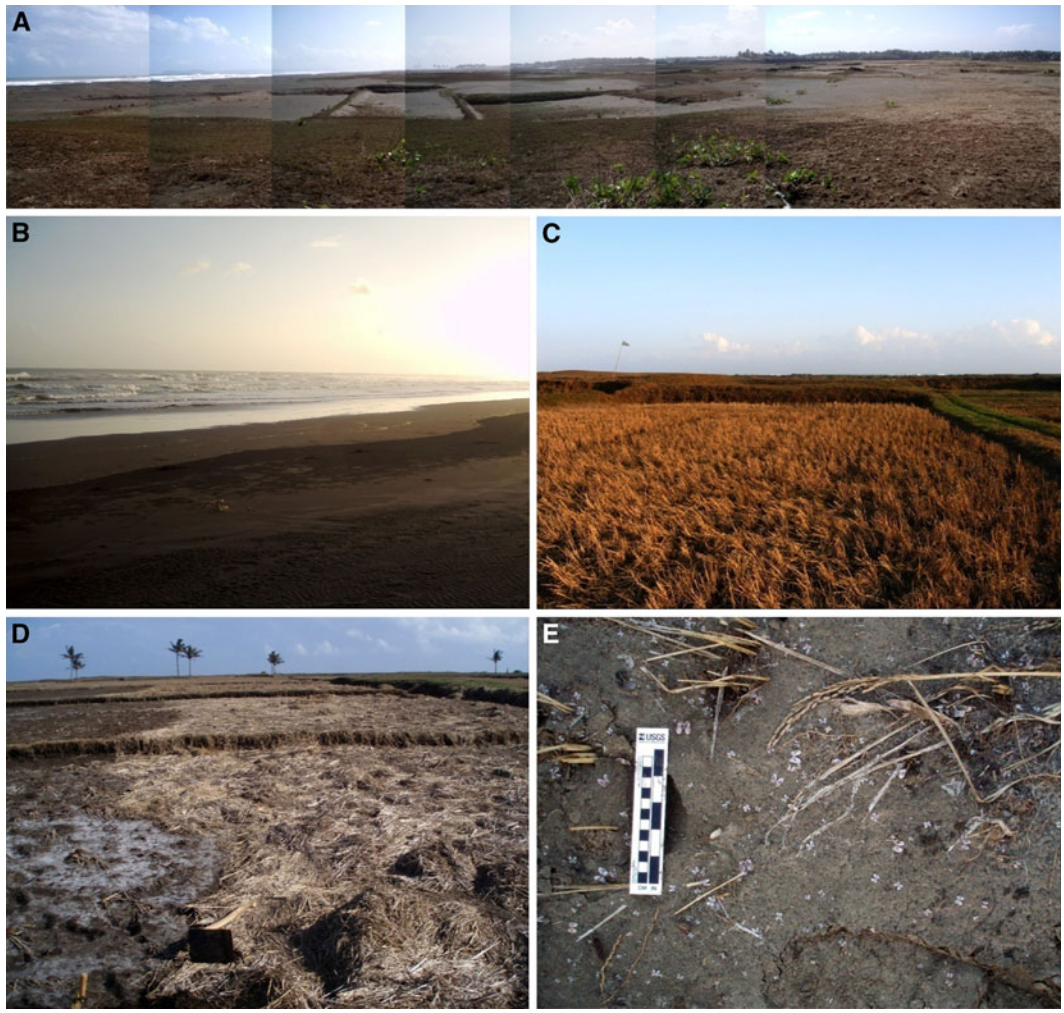

Figure 5
Views of the sediment transect about 3 weeks after the tsunami. **a** Panorama looking west about 200 m west of transect, showing general topography of the area. **b** Shoreline at the transect showing relatively flat shoreline and spilling breakers. **c** View shoreward along the transect showing rice plants bent over in the direction of flow (here, locally eastward in an overall northward flow). **d** View shoreward from ~600 m along transect showing rice plant debris piled up on downwind part of rice paddies, suggesting that water was impounded here. **e** Tsunami deposit surface ~150 m along transect showing abundant articulated *Donax* shells at the surface; these shells were not common elsewhere and suggest that a colony was emplaced as a group

We saw no direct evidence of tsunami-induced erosion on the transect. The beach has no visible scarp, and even in our most seaward study location, rice plants are still rooted in soil (Fig. 5c). The boundary between the tsunami deposit and the underlying soil is sharp, but retains fine details such as footprints, further suggesting that little erosion occurred on the transect.

The tsunami deposit overlies a brown (7.5 YR 4/4) sandy soil made up of sands mineralogically similar to those of the tsunami deposit, but finer grained (see photographs in Fig. 3). The soil also contains silt and clay not found in the beach sediments; the coarse silts are organic-rich, and probably represent organic debris from rice cultivation, mixed with breakdown products of the iron oxides. The clay fraction is inorganic, and is probably iron oxide pigments. The presence of clays is likely to be partially responsible for the lack of erosion of this basal soil.

Along the transect, the tsunami deposit itself changes little in color (black, 7.5 YR 2.5/1; photographs in Fig. 3). Between the coastline and 350 m inland (T10), it is a moderately sorted medium sand becoming a poorly sorted fine to very fine sand landward, with some fluctuations in mean grain size between 550 and 700 m (samples T16 through T26; Fig. 3). The sand grains are primarily olivine, magnetite, and ilmenite ($\sim$70%), with minor amounts of quartz, amphibole, lithics, and glass. The grains are generally angular, although olivine and quartz grains are often subrounded as well. Although the overall lithology is monomodal, lithics make up the bulk of the coarser grains, and oxides the bulk of the finer grains, suggesting that the hydraulic sorting based on changes in density is perhaps more representative than our grain sizing techniques. The prominence of iron oxides is supported by the measured high sediment density (3.54 g/cm^3), which is consistent with mixing siliciclastic grains and magnetite/ilmenite. Few shells or coral fragments were found in the deposit, but in at least one location (150 m from shore), hundreds of articulated *Donax* shells were found at the surface, suggesting that a displaced colony failed to adapt to life on land (Fig. 5d).

The tsunami deposit maintains a thickness of between 10 and 20 cm from where it first becomes discernable from the underlying sediment 70 m from the shoreline (T1–T10; Fig. 3). At 330 m from the shoreline, the deposit begins to thin, becoming only 1.5 cm by 440 m, and only 0.1 cm by 470 m (T11–T14). The deposit continues as a layer a few grains thick until 720 m, when it again becomes indistinguishable from the underlying soil (T15–T26). A wrack line of floated, organic material suggests that inundation continued for 40 m past the last depositional evidence, a total of 755 m from shore. Deposition is typically thicker on the landward side of the flow-normal paddy dikes closer to the beach (e.g., T3–T11)—in more landward sections, debris (and some sediment) has been piled up against the rear dikes of the paddies, suggesting that floating debris was pushed back by the prevailing sea breeze (Fig. 5e).

Seaward parts of the deposit are plane laminated throughout (samples T1–T7), but the laminae were not detectable by 200 m from shore. Sand between 200 and 400 m from shore had dried sufficiently in the 3 weeks since deposition that it was not possible using the techniques available to determine if any structures had been preserved as sand typically fell away to the angle of repose when cut into. In the very seaward portions of the deposit (T1–T3, from 70 to 115 m), two bands of blacker sand containing more magnetite than usual for the deposit appear at the base and about halfway up the deposit. These bands become indistinct farther landward, but density changes in a core taken 160 m from shore suggest that the bands persist at least that far inland (Fig. 6).

Lateral changes of mean sediment grain size analysis along the transect shows overall landward fining, with more variable lateral grain size trends as the deposit tapers off (Fig. 3). Mean grain size along the transect remains constant at just coarser than 2 Φ (0.25 mm) from at least 70 to 350 m along the transect (T1–T10), then begins to fine smoothly, reaching 3.75 Φ (0.075 mm) by T16 at 550 m (Fig. 3). From 550 m (T17) to the end of deposit, however, mean grain size becomes variable, although it never becomes as coarse as the seaward part of the transect.

Vertical changes in grain size are also variable. Upward fining takes place in two distinct pulses where measured, 100 m from shore (near T2; Fig. 6). From the base of the sand to about 1/3 of the deposit thickness (here 4.5 cm) the sand is inversely graded, coarsening upwards from 1.7 Φ (0.3 mm) to 1.3 Φ (0.38 mm). The second third of the deposit (between 4.5 and 9.5 cm) fines upwards (normally graded), returning the mean grain size to 1.7 Φ (0.3 mm). The uppermost third (9.5–15 cm) repeats the inversely graded/normally graded pattern, but only coarsens to 1.6 Φ (0.33 mm) before falling to 2 Φ (0.25 mm). Sediment bulk density generally behaves inversely to grain size (so that the coarsest grains are the least dense), but the density changes are not sufficient to make the finer grains hydraulically equivalent to the coarser ones, so that grain size patterns in the deposit represent changes in hydraulics and not density sorting of hydraulically equivalent grains.

The grain size population of the tsunami deposit suggests at least four modes that may well represent different sediment sources. The coarsest mode, centered near 1.5 Φ (see grain size distribution of T5, Fig. 3), is moderately well sorted and similar to

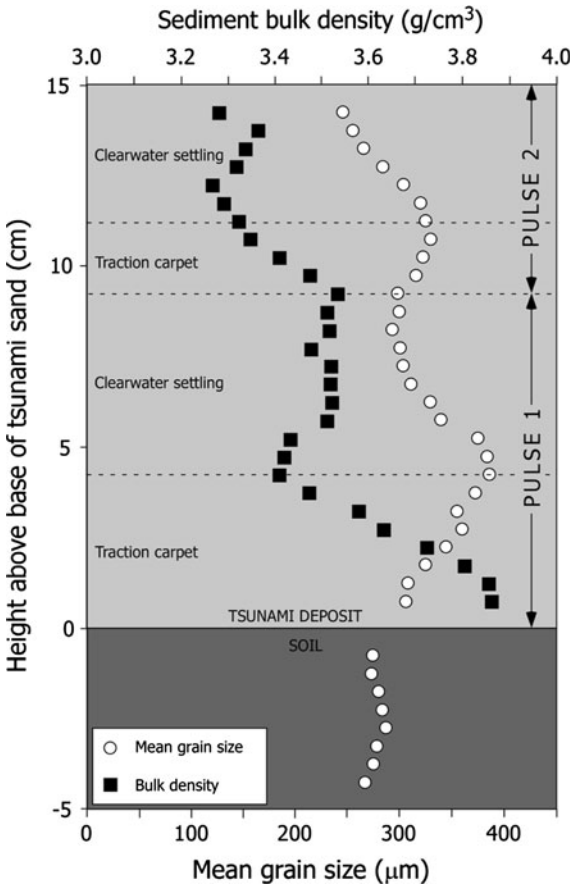

Figure 6
Vertical grain size and density changes in a core taken 100 m from shore. *Points* plotted are a three-point moving average of measured values to help make trends in size and density more visible; as a result, the plotted data stop one datapoint away from each boundary

sediments collected from the present shoreline (black curve in distribution seen in Fig. 3). This mode is prominent in sediments low in the deposit, and from the seaward part of the deposit (up to 250 m from the shore-T1 through T8). The next finer mode, centered near 1.75 Φ, is also moderately well sorted, and similar to the coarsest mode found in paddy soils underlying the tsunami deposit. This mode is prominent in sediments found higher in the deposit, and from the landward part of the deposit (from about 250 m from shore (T9) to the edge of deposition). Two finer modes centered at 5 and 8 Φ are noted as the skewness and sorting of the grain size distribution increases as seen in samples T14 and T25, higher and landward in the deposit. They are also similar to modes found in paddy soils in the area.

6. Interpretation

The sedimentary evidence from the 2006 tsunami at Adipala reflects the eyewitness observations of two waves, each waning with time and distance inland. Lateral trends in grain size suggest that most of the ocean-derived sediment had been deposited by ~450 m from shore. The marked thinning of the deposit landward of 450 m results from a change from relatively plentiful ocean sediment to relatively scarce, difficult to erode, and more clayey paddy sediment landward. Vertical trends in grain size reveal more complexity than simple settling from two pulses of sediment, and suggest the existence of a traction carpet at the base of each wave.

6.1. Lateral Grain Size Changes

The lateral grain size changes in Fig. 3 show that from the shore line to at least 350 m from shore (sample T10), the tsunami sand is very similar to beach sand, although somewhat finer, less sorted, and more positively skewed (see T5 grain size distribution). By 450 m from shore (T12), however, the tsunami sand has become much less sorted, with a dominant mode consistent with the underlying soil. This suggests that beach sediments were picked up and moved landward, and by 450 m inland, the tsunami had effectively run out of beach sediments having deposited all that was available, although it was still capable of moving sediments (as evidenced by the sediment of similar grain size still present 450 m inland). Advection inland is also suggested by colonies of living *Donax* transported inland and found in distinct groups in the tsunami sediment 150 m inland along the transect.

The two finest modes in the tsunami deposit (centered at 5 and 8 Φ) are inferred to be from soil, and are most prominent in fine sediment drapes along the transect inland from 450 m (where the tsunami ran out of beach sediment to deposit), although they are found throughout the transect. These sediments are so fine grained that their presence in the tsunami sediment implies that water pooled for some time over most of the transect that allowed fine sediments to settle out of suspension. The prominence in landward parts of the transect is probably because

little sandy sediment remained to be deposited here—as a result, the finer fraction becomes relatively more important. Dikes between the rice fields would have acted as impediments to shallow flow eventually leading to impoundment and pooling at the landward end of the transect.

6.2. Vertical Grain Size Changes

The core 100 m from shore shows two sequences of a coarsening upward trend at the base followed by a fining upward trend (Fig. 6). The coarsening upwards layers also show high density sediment to the base, and become less dense upward, whereas the fining upwards layers remain relatively constant with respect to density. The layers that fine upwards are easily explained as the product of suspended sediment settling from a decelerating flow, as might be expected from a tsunami. The coarsening upwards deposits, however, are more unusual.

The observed inverse correlation of density and grain size suggests kinetic sieving, where collisions at the base of the flow cause finer grained and denser material to fall downwards as the larger, less dense grains are jostled to the top (Sohn, 1997). This highly concentrated sediment at the base of the flow is known as a "traction carpet," or a collision-dominated flow driven by high shear stresses in the suspension-dominated flow above. As the bed aggrades, the first grains deposited (smallest, most dense) become selectively removed from the traction carpet. These particles are less dense than the larger particles and their absence explains the reduction in the overall bulk density upward in the deposits (Fig. 6).

Based on the coarsening upward trends in the base of the deposit, deposition during the tsunami occurs as a thin, hyperconcentrated flow of beach sand at the base of the tsunami and a thick, turbulent flow that keeps particles in suspension as the tsunami flows across land (LeRoux and Vargas, 2005). The hyperconcentrated "traction carpet" exists because of very high shear rates in the overlying flow, and can be maintained only as long as those shear rates remain high. During the lifespan of the traction carpet, material settling to the bed from the turbid flow enters the traction carpet, providing more sediment to that flow. Once shear in the overlying flow drops to the extent that the traction carpet can no longer be maintained, normal settling begins, producing a normally graded bed. Passage of a second wave repeats the process.

Traction carpets do not sort sediment laterally. Landward fining from the suspended sediment portion of the flow will be obscured where the carpet is present. Landward fining at Adipala does not begin until about 300 m, suggesting that the traction carpet extends about this far inland.

6.3. Size Estimate

Size of the tsunami can be estimated using the coarsest grains deposited by the turbid portion the flow (as compared to those in the traction carpet), the distance from shore where they were found, then testing against field evidence of tsunami height. If the beach sands found in the tsunami deposit were to have traveled in suspension from their source (at or near the shoreline) to the farthest distance inland at which they were found, the maximum time available for travel is the time it would take for these grains to settle from the top of the flow, a time given by:

$$\frac{h}{w_s} = t = \frac{l}{U} \tag{1}$$

where w_s is the settling velocity of the coarsest grains, h is the depth of the flow, U is the depth-averaged velocity, and l is the distance from the beach ridge to the location of the last grains (Moore, 1994; Moore *et al.,* 2007). The coarsest grains present 350 m inland measure about 1.1 Φ (0.48 mm at T10); using the average sediment bulk density for sediments in the turbid part of the flow (~ 3.4 g/cm^3), the settling velocity of these grains is 8.0 cm/s (Dietrich, 1982). Substituting into Eq. 1 yields:

$$Uh = 28 \tag{2}$$

for this flow. If the tsunami arrived as a bore (as eyewitnesses report), then the Froude number of the wave should be at or near 1 (Fritz *et al.,* 2003)

$$F = \frac{U}{\sqrt{gh}} \approx 1 \tag{3}$$

which yields a two-equation, two-unknown system. Solving this system using the method outlined in

Moore *et al.,* (2007) gives a flow depth of about 4.3 m moving at 6.5 m/s for the first wave of the tsunami. Using a slightly subcritical Froude number (as should occur in the area just seaward of the bore, where most sediment transport will occur) of 0.8 yields a flow depth of 5.0 m moving at 5.6 m/s, which correlates well with the field observations of a 5 m tsunami in this area (Fritz, *et al*., 2006).

It should be noted that the modeling of tsunami flow velocity from particle advection described above has three main assumptions. First, that the largest grain size is suspended to the top of water column. Second, that such a particle falls from that height to the bed at the landward limit that the particle is found without multiple up and down excursions, possibly hitting the bed and being resuspended. The effect of violation of the second assumption is that the effective settling velocity is lower than the actual settling velocity and that the flow velocity is lower than that calculated using the water column height at the shore. Third, that the velocity at the shore applies for the entire transport path to 350 m, where the sediment particle was deposited. This is an overestimate if the tsunami slows as it moves inland, which is typical.

7. Summary

Along a 750-m-long transect of sediments deposited by the 2006 Central Java tsunami near Adipala, Indonesia, sandy deposits show a zone of little landward fining from 0 to 300 m, where the deposit is thickest. From 300 to 500 m inland, the deposit fines landward but becomes dramatically thinner. From 500 m landward to the limit of deposition, a very thin deposit shows inconsistent grain sizes, most likely caused by the mixture of fine silt and clay from the tsunami deposit mixed during sampling with underlying soil. Vertical trends in the sand show two coarsening-fining upward cycles, probably corresponding to the two waves reported by eyewitnesses. The coarsening base of each pulse probably represents a traction carpet caused by high excess shear in the overlying tsunami. When parameterizing, fining by the change in bulk (deposit averaged) grain size including portions deposited by traction carpets obscure trends in landward fining, since little to no lateral grain size trend is to be expected in this transport mode. Having two modes of sediment transport (traction carpet and suspended sediment) also tends to complicate modeling based on sediment thickness, as they hyperconcentrate part of the flow, making a thicker deposit than would a wave without a traction carpet. On the other hand, the overall thickness and distance inland traveled by traction carpets may provide insight into tsunami hydraulics, adding to information available from the turbid portion of the deposit. It is probable that high sediment bulk density at the site created favorable conditions for the formation of a traction carpet. Data from subsequent post-tsunami surveys, however, will help to clarify this proposition.

References

Asikin, S., Handoyo, A., Prastistho, B., and Gafoer, S., 1992, Geology of the Banyumas Quadrangle, Java: Bandung, Indonesia, Geological Research and Development Center, Department of Mines and Energy.

Bahlburg, H., and Weiss, R., 2007, *Sedimentology of the December 26, 2004, Sumatra tsunami deposits in eastern India (Tamil Nadu) and Kenya*: International Journal of Earth Sciences, vol. *96*, no. 6, p.1195-1209.

Bilek, S.L., and Engdahl, E.R., 2007, *Rupture characterization and aftershock relocations for the 1994 and 2006 tsunami earthquakes in the Java subduction zone*. Geophys. Res. Lett., *34*, L20311, doi:1029/2007GL031357.

Dawson, A.G., Shi, S., Dawson, S., Takahashi, T., and Shuto, N., 1996, *Coastal sedimentation associated with the June 2nd and 3rd, 1994 tsunami in Rajegwesi, Java*: Quaternary Science Reviews, v. *15*, p. 901-912.

Dietrich, W.E., 1982. *Settling velocity of natural particles*. Water Resources Research *18*, 1615–1626.

Dominey-Howes, D., and Thaman, R., 2009, UNESCO-IOC International Tsunami Survey Team Samoa (ITST Samoa) Interim Report of Field Survey, 14th Ð 21st October 2009. Australian Tsunami Research Centre Miscellaneous Report No. 2: October 2009, 190 p.

Fritz, H.M., J.C. Borrero, C.E. Synolakis, J. Yoo, 2006, *2004 Indian Ocean tsunami flow velocity measurements from survivor videos*, Geophys. Res. Lett., *33*, L24605, doi:10.1029/2006GL026784.

Fritz, H.M., Hager, W.H., Minor, H.-E., 2003, *Landslide generated impulse waves: part 1: instantaneous flow fields*. Exp. Fluids *35*:505-519.

Fritz, H.M., W. Kongko, A. Moore, B. McAdoo, J. Goff, C. Harbitz, B. Uslu, N. Kalligeris, D. Suteja, K. Kalsum, V. Titov, A. Gusman, H. Latief, E. Santoso, S. Sujoko, D. Djulkarnaen, H. Sunendar, C. Synolakis, 2007, *Extreme runup from*

the 17 July 2006 Java tsunami, Geophys. Res. Lett., *34*, L12602, doi:10.1029/2007GL029404.

Fujii, Y., and Satake, K., 2006, *Source of the July 2006 West Java tsunami estimated from tide gauge records*, Geophys. Res. Lett., *33*, doi:10.1029/2006GL028049.

Gelfenbaum, G., and Jaffe, B., 2003, *Erosion and sedimentation from the 17 July, 1998 Papua New Guinea tsunami*: Pure and Applied Geophysics, v. *160*, p. 1969-1999.

Jaffe, B., and Gelfenbaum, G., 2007, *A Simple Model for Calculating Tsunami Flow Speed from Tsunami Deposits*: Sedimentary Geology, v. *200*, p. 347-361.

LeRoux, J.P., and Vargas, G., 2005, *Hydraulic behavior of tsunami backflows: insights from their modern and ancient deposits*: Environmental Geology, v. *49*, p. 65-75.

Minoura, K., Imamura, F., Takahashi, T., and Shuto, N., 1997, *Sequence of sedimentation processes caused by the 1992 Flores tsunami*: Geology, v. *25*, p. 523-526.

Moore, A., 1994, Evidence for a Tsunami in Puget Sound ~1000 Years Ago [M.S. thesis]: Seattle, University of Washington.

Moore, A., McAdoo, B.G., and Ruffman, A., 2007, *Landward fining from multiple sources in a sand sheet deposited by the 1929 Grand Banks tsunami, Newfoundland*: Sedimentary Geology, v. *200*, p. 336-346.

Moore, A., Nishimura, Y., Gelfenbaum, G., Kamataki, T., and Triyono, R., 2006, *Sedimentary deposits of the 26 December 2004 tsunami on the northwest coast of Aceh, Indonesia*: Earth, Planets, and Space, v. *58*, p. 253-258.

Newman, A. V., and E. A. Okal, 1998, *Teleseismic estimates of radiated seismic energy: The E/M0 discriminant for tsunami earthquakes*, J. Geophys. Res., *103*(11), 26,885–26,898.

Nishimura, Y., and Miyaji, N., 1995, Tsunami deposits from the 1993 Southwest Hokkaido earthquake and the 1640 Hokkaido Komagatake eruption, Northern Japan, *in* Satake, K., and Imamura, F., eds., Tsunamis: 1992-1994, their generation, dynamics, and hazard: Basel, Birkhäuser, p. 719-734.

Paris, R., Wassmer, P., Sartohadi, J., Lavigne, F., Barthomeuf, B., Desgages, E., Grancher, D., Baumert, P., Vautier, F., Brunstein, D., and Gomez, C., 2009, *Tsunamis as geomorphic crises: Lessons from the December 26, 2004 tsunami in Lhok Nga, West Banda Aceh (Sumatra, Indonesia)*: Geomorphology, *104*, 59-72.

Reymond, D., and E. A. Okal, 2006, *Rapid, yet robust source estimates for challenging events: Tsunami earthquakes and mega-thrusts, Eos Trans. AGU*, *87*(52), Fall Meet. Suppl., Abstract S14A-02.

Sato, H., Shimamoto, T., Tsutsumi, A., and Kawamoto, E., 1995, Onshore tsunami deposits caused by the 1993 Southwest Hokkaido and 1983 Japan Sea earthquakes, *in* Satake, K., and Imamura, F., eds., Tsunamis: 1992-1994, their generation, dynamics, and hazard: Basel, Birkhauser, p. 693-717.

Shi, S., Dawson, A.G., and Smith, D.E., 1995, Coastal sedimentation associated with the December 12th, 1992 tsunami in Flores, Indonesia, *in* Satake, K., and Imamura, F., eds., Tsunamis: 1992-1994, their generation, dynamics, and hazard: Basel, Birkhauser, p. 525-536.

Sohn, Y.K., 1997, *On traction-carpet sedimentation*: Journal of Sedimentary Research, v. *67*, p. 502-509.

(Received September 8, 2010, revised December 28, 2010, accepted December 29, 2010, Published online May 4, 2011)